Vibro-acoustical modal analysis: Reciprocity, model symmetry, and model validity

Katrien Wyckaert
LMS International, Interleuvenlaan 68, 3001 Leuven, Belgium

Fülöp Augusztinovicz and Paul Sas
Mechanical Engineering Department, Division PMA, Katholieke Universiteit Leuven, Celestijnenlaan 300B, 3001 Leuven, Belgium

(Received 22 December 1994; accepted for publication 4 April 1996)

For low-frequency applications, a modal approach can be useful to describe vibro-acoustical coupling. Based on combined vibrational/acoustical frequency response function measurements, either with respect to acoustical or structural excitation, modal vibro-acoustical analysis can be carried out. This paper presents a consolidation of the theory behind the vibro-acoustical modal model. The model formulation is shown to be a nonsymmetrical formulation. It is shown that this is not contradictory to the well-known vibro-acoustical reciprocity principle. The implications of the nonsymmetry for the modal model are discussed. It is pointed out which variables must be measured and what kind of scaling must be used in order to end up with a consistent modal formulation. The theory is illustrated and verified by measurements on an experimental vibro-acoustical system, consisting of a rigid cavity with one flexible wall.

PACS numbers: 43.40.Rj, 43.20.Tb, 43.20.Ks, 43.58.Vb [CCB]

LIST OF SYMBOLS

c	speed of sound in fluid (m/s)
i	$\sqrt{(-1)}$
p	sound pressure (N/m^2)
q	volume velocity (m^3/s)
s	Laplace variable
S_b	flexible boundary of the acoustical cavity (m^2)
x	structural displacement (m)
f	structural (point) force (N)
ρ	fluid density (kg/m^3)
ω	angular frequency (rad/s)
A^s	system matrix of structural subsystem
A^f	system matrix of fluid subsystem
C^s	structural damping matrix
C^f	fluid damping matrix
K^s	structural stiffness matrix
K^f	fluid stiffness matrix
M^s	structural mass matrix
M^f	fluid mass matrix
K^c	coupling submatrix, representing the effect of fluid on structure
M^c	coupling submatrix, representing the effect of structure on fluid
$\{f\}$	vector of external force loading on structure
$\{q\}$	vector of acoustical source loading on fluid
$\{l_p\}$	vector of fluid pressure loading on structure
$\{l_f\}$	vector of structural loading on fluid
B	system matrix of coupled system (Laplace domain)
H	transfer function matrix (Laplace domain)
λ	eigenvalue of the system matrix B
$\{\psi\}$	eigenvector of the system matrix B
A_r	residue matrix
$\{\mathbf{n}\}$	surface normal vector
$\{\mathbf{n}_i\}$, $\{\mathbf{n}_j\}$	interpolation function vector
$\|X\|$	determinant of matrix X
adj(X)	adjoined of matrix X

INTRODUCTION

When considering the global vibro-acoustical problem of real-life enclosures, coupling is often found to exist between the acoustical response in the cavity and the structural excitation, whereas the structural response is also related to acoustical excitation sources in the cavity. Car interiors, cabs of trucks, and aircraft fuselages are just a few practical examples of this sort of system. Coupling implies that the acoustical and vibrational system behavior are not independent from each other, and therefore the global system behavior has to be considered as one unit.

With the ever increasing interest in these fluid–structure interactions, numerous analysis techniques have been developed and published so far. Some early investigations have dealt with the problems of a vibrating plate backed by a rigid enclosure by using analytical and experimental methods.[1–4] A detailed theoretical treatment of fluid–structure interactions, based on the modal expansion theory and extended by experimental verification, has been given by Dowell *et al.*[5] and by Pan and Bies.[6,7] Numerical techniques, originally developed for mechanical systems, have been adopted and applied for acoustical and vibro-acoustical systems, as summarized recently by Göransson[8] and Coyette.[9]

In order to fully understand and model the vibro-acoustical problem, modal analysis can also be considered, which aims at identifying an (interdependent) modal model

for the vibrational and acoustical part of the system in the lower-frequency range. Based on mechano-acoustical analogies, the adoption of mechanical experimental modal analysis procedures for the case of pure acoustical systems is rather straightforward[10–13] and has been known for quite some time now. Similarly, numerical modal synthesis techniques are also in use for vibro-acoustical systems.[14,15] However, only a few papers have been published on the theoretical[16] and experimental[17] modal analysis of vibro-acoustical systems.

As will be discussed below in detail, the modal analysis of mixed vibro-acoustical systems is burdened by a number of theoretical and practical problems. First of all, in order to devise a consistent modal formulation, the correct physical quantities need to be measured, and it is important to understand how the applied quantities relate to each other. The issue of selecting appropriate variables inevitably poses questions concerning the nonsymmetry of the vibro-acoustical model, which in turn might seem to be in contradiction with the unquestionable reciprocity of vibro-acoustical systems. All of these matters have repercussions on the choice of the excitation method, which can in principle be either acoustical or structural.

The aim of this paper is to summarize the theory behind a possible, relevant vibro-acoustical modal model. Unlike the modal expansion techniques, the treatment is based on spatial discretization techniques which are usual in the numerical analysis of dynamic systems. It will be shown that using easily or reasonably measurable quantities, such as force and volume acceleration, as excitation, and sound pressure and surface displacement, as response variables, results in a nonsymmetrical matrix equation. Due to the special nature of this nonsymmetry, the right and left eigenvalues of the system matrix are different but closely related, and thus the left eigenvalues can easily be derived which otherwise would not be amenable to experimental analysis. The implications of the established relationships for experimental vibro-acoustical modal analysis are outlined and the theory is verified on a simple model measurement.

I. MODEL FORMULATION

In order to understand the equations describing the vibro-acoustical behavior of coupled systems, one can start with the finite element formulations.[8] The (finite element) equation of motion for the structural vibrational behavior under external structural loading, as well as under coupled acoustical loading, is as follows:

$$[-\omega^2 M^s - i\omega C^s + K^s]\{x\} = \{f\} + \{l_p\}, \tag{1}$$

$$\{l_p\} = \int_{S_b} p \, dS. \tag{2}$$

Equation (2) represents the acoustical pressure loading on the structure over the boundary surfaces S_b of the cavity.

On the other hand, when considering the acoustical problem, the acoustical pressure response in the cavity is caused by acoustical excitation, as well as by structural vibration on the boundaries. From the indirect acoustical formulation, the following equation can be derived for the fluid:

$$[-\omega^2 M^f - i\omega C^f + K^f]\{p\} = \rho\{\dot{q}\} + \omega^2\{l_f\}, \tag{3}$$

$$\omega^2\{l_f\} = \omega^2 \int_{S_b} \rho x_N \, dS. \tag{4}$$

The matrices M^f, C^f, and K^f describe the pressure–volume acceleration relation in case of a rigid wall structure. These matrices do not reflect directly physical properties of the fluid, but result from an indirect formulation of the acoustical problem. Equation (4) represents the loading due to (normal) vibration x_N at the flexible boundary S_b of the cavity.

Rewriting and combining Eqs. (1), (2), (3), and (4) results in the following description of the vibro-acoustical coupled system:

$$\begin{bmatrix} K^s & -K^c \\ 0 & K^f \end{bmatrix}\begin{Bmatrix} x \\ p \end{Bmatrix} - i\omega\begin{bmatrix} C^s & 0 \\ 0 & C^f \end{bmatrix}\begin{Bmatrix} x \\ p \end{Bmatrix} - \omega^2\begin{bmatrix} M^s & 0 \\ M^c & M^f \end{bmatrix} \times \begin{Bmatrix} x \\ p \end{Bmatrix} = \begin{Bmatrix} f \\ \rho\dot{q} \end{Bmatrix}. \tag{5}$$

From (2) and (4) it can be seen intuitively that M^c and K^c are related to each other. Indeed, according to Göransson,[8] the elements of the matrices K^c and M^c can be expressed as follows:

$$K^c_{ij} = \int_{S_b} \{\mathbf{n}_i\}\{\mathbf{n}\}\mathbf{n}_j \, dS, \tag{6}$$

$$M^c_{ji} = \int_{S_b} \rho \mathbf{n}_i\{\mathbf{n}_j\}\{\mathbf{n}\} \, dS, \tag{7}$$

where $\{\mathbf{n}\}$ is the surface normal vector and $\{\mathbf{n}_i\}$ is the interpolation function vector in the finite element formulation. This indicates that both matrices are (in a transposed form) interrelated with a factor of ρ, the fluid density:

$$M^c = \rho K^{c^t}. \tag{8}$$

The set of equations (5) represents a second-order model formulation for the vibro-acoustical behavior and can be used as a basis for further deduction. However, it is clear that the set of equations is nonsymmetrical. This is even more clear when rewriting Eq. (5) into a more compact matrix form:

$$\begin{bmatrix} A^s & -K^c \\ -\omega^2 M^c & A^f \end{bmatrix}\begin{Bmatrix} x \\ p \end{Bmatrix} = \begin{Bmatrix} f \\ \rho\dot{q} \end{Bmatrix}, \tag{9}$$

with

$$A^s = K^s - i\omega C^s - \omega^2 M^s,$$
$$A^f = K^f - i\omega C^f - \omega^2 M^f. \tag{10}$$

II. VIBRO-ACOUSTICAL RECIPROCITY

Reciprocity in structural problems, as well as in acoustical problems, is well known. In the structural case, acceleration response and force are related, while in the acoustical case, volume acceleration and pressure are related. For vibro-acoustical coupled problems, the vibro-acoustical reciprocity principle is valid. As formally demonstrated first by Lyamshev,[18] followed by Ten Wolde *et al.*,[19] Fahy,[20] and

recently by Norris and Rebinsky,[21] the most usual form of vibro-acoustical reciprocity is expressed as follows:

$$\left.\frac{p_i}{f_j}\right|_{\dot{q}_i=0} = \left.\frac{-\ddot{x}_j}{\dot{q}_i}\right|_{f_j=0}. \tag{11}$$

In words, the ratio between the acoustical response p_i at response location i within a cavity and a structural force excitation f_j at location j on the structure (without excitation by an acoustical source) equals the ratio between the acceleration response $\ddot{x}_j$ measured at the location and in the direction of the applied force j and acoustical excitation (expressed in volume acceleration of an ideal monopole) $\dot{q}_i$ at the pressure measurement location i (in absence of structural excitation). Even if this is not obvious at first glance, this basic reciprocity principle is also reflected in the set of Eq. (9) which describe the coupled vibro-acoustical problem, as will be shown below.

When only structural excitation and no acoustical excitation is applied ($!f;\dot{q}=0$), it can be deduced from (8) and (9):

$$\left.\frac{p_i}{f_j}\right|_{\dot{q}_i=0} = \left[A^s \frac{K^{c^t{}^{-1}}}{\rho\omega^2} A^f - K^c\right]^{-1}_{ij}. \tag{12}$$

Similarly, when only acoustical excitation is applied ($!\dot{q};f=0$):

$$\left.\frac{\ddot{x}_j}{\dot{q}_i}\right|_{f_j=0} = \left[K^{c^t} - A^f \frac{K^{c^{-1}}}{\rho\omega^2} A^s\right]^{-1}_{ji}. \tag{13}$$

When the submatrices A^s, A^f, and K^c are symmetrical (which is *a priori* met under a linear assumption), the reciprocity relation (11) can be deduced from this set of equations. The importance of Eq. (9) lies in the fact that vibro-acoustical reciprocity is valid, even if the describing set of equations is not symmetrical. The nonsymmetry of Eq. (9) is a particular feature of coupled vibro-acoustical systems, described by means of the used formulation. It differs both from the full symmetry of the governing equations of purely mechanical or acoustical systems, where reciprocity is expressed by symmetrical matrices, and also from the skew symmetrical, "gyroscopic" coupling terms of those matrix equations, obtained from the modal expansion method.[5,6] In other words, the intrinsic and more general feature of reciprocity of physical systems is not necessarily accompanied by full symmetry in the mathematical descriptions. Similar conclusions have been drawn, even though in a somewhat different context, recently by other authors.[22–24]

It is worth noting that the nonsymmetrical formulation of the set of equations is due to the choice of variables x, p, f, and $\dot{q}$, which is imperative to arrive at the formulation described in Eq. (9). By using another set of variables (e.g., x, f, p, and $\int q$), the term ω^2 appears together with A^f rather than with M^c in Eq. (9), rendering the equation symmetrical. In order to end up with a symmetrical set of equations, and thus enable the analyst to use efficient solvers in finite element analysis of vibro-acoustical systems, the introduction of a further unknown, i.e., mainly some sort of fluid potential, is usual.[25–27] However, this formulation does not have the required harmonic form to be used in standard experimental modal analysis (EMA) techniques. To the authors' knowledge, no formulation has been put forward which is symmetrical, corresponds to the presently used EMA formulation, and at the same time uses easily measurable acoustical parameters.

III. IMPLICATIONS FOR THEORETICAL VIBRO-ACOUSTICAL MODAL ANALYSIS

From the set of Eqs. (5), it is clear that both the acoustical uncoupled problem and the vibrational uncoupled problem ($K^c, M^c=0$) can be described by a symmetrical set of second-order equations. The same type of modal parameter estimation and modal decomposition algorithms used for uncoupled vibrational problems can thus be used for uncoupled acoustical problems. Linearity is always assumed, also requiring linear damping models.

For the vibrational uncoupled problem, (measured) transfer characteristics x/f (displacement over force) are equivalent to the transfer characteristics $p/\dot{q}$ (acoustical pressure over volume acceleration of the acoustical sources) for the uncoupled acoustical problem.

For the coupled problem, ($K^c, M^c \neq 0$), the set of second-order equations (9) can be rewritten, based on (8) as:

$$\begin{bmatrix} A^s & -K^c \\ -\omega^2 K^{c^t} & A^f/\rho \end{bmatrix} \begin{Bmatrix} x \\ p \end{Bmatrix} = B \begin{Bmatrix} x \\ p \end{Bmatrix} = \begin{Bmatrix} f \\ \dot{q} \end{Bmatrix}. \tag{14}$$

Conforming to general modal analysis theory,[28] it follows that a transfer function matrix $H(s)$ can be written as:

$$H(s) = B(s)^{-1}, \tag{15}$$

with, based upon standard matrix calculation,

$$B(s)^{-1} = \frac{\text{adj}(B(s))}{|B(s)|}, \tag{16}$$

$$\text{adj}(B(s)) = [\epsilon_{ij}|B_{ij}|]^t, \tag{17}$$

with $|B_{ij}|$ the determinant of $B(s)$ without row i and column j; $\epsilon_{ij}=1$ if $i+j$ is even, and $\epsilon_{ij}=-1$ if $i+j$ is odd.

With λ_r the roots of the characteristic system equation $|B(s)|=0$, and by applying the theory of partial fraction expansion, (15) can be rewritten as

$$H(s) = \frac{\text{adj}(B(s))}{E\Pi_{r=1}^{N}(s-\lambda_r)(s-\lambda_r^*)} = \sum_{r=1}^{N} \frac{A_r}{(s-\lambda_r)} + \frac{A_r^*}{(s-\lambda_r^*)}, \tag{18}$$

with E a constant, N the number of modes in the frequency band of interest, and A_r the so called residue matrix. The residues equal

$$A_r = P_r \cdot \text{adj}(B(\lambda_r)) \tag{19}$$

with P_r a pole-dependent constant.

By right multiplication and by left multiplication with $B(s)$, Eq. (16) can be rewritten as

$$\text{adj}(B(s)) \cdot B(s) = |B(s)| I, \tag{20}$$

$$B(s)\cdot \mathrm{adj}(B(s)) = |B(s)|I. \tag{21}$$

Evaluating Eqs. (20) and (21) at eigenvalues λ_r shows that, since λ_r is a root of the characteristic equation, the left and the right eigenvalues are proportional to the adjoined matrix:

$$\{\psi_l\}^t \cdot B(\lambda_r) = \mathrm{adj}(B(\lambda_r))B(\lambda_r) = 0, \tag{22}$$

$$B(\lambda_r)\cdot\{\psi_r\} = B(\lambda_r)\mathrm{adj}(B(\lambda_r)) = 0. \tag{23}$$

Considering any arbitrary row of Eq. (22) or any arbitrary row of Eq. (23) shows that each row of the adjoined matrix is proportional to the left eigenvector ψ_l and that each column of the adjoined matrix is proportional to the right eigenvector ψ_r. Note that in case of a nonsymmetrical system the left and right eigenvalues are different from each other.

For the special nonsymmetry of system Eq. (14), it can be proven that the right and the left eigenvectors show a special relation with respect to each other. Let the right eigenvectors be named

$$\begin{Bmatrix} \psi_{sr} \\ \psi_{fr} \end{Bmatrix},$$

then the left eigenvectors

$$\begin{Bmatrix} \psi_{sl} \\ \psi_{fl} \end{Bmatrix}$$

can be written as (subscript s is indicative for the structural response locations, subscript f for the acoustical fluid response locations):

$$\begin{Bmatrix} \psi_{sl} \\ \psi_{fl} \end{Bmatrix}_{\lambda_r} = \begin{Bmatrix} \psi_{sr} \\ \dfrac{1}{\lambda_r^2}\psi_{fr} \end{Bmatrix}_{\lambda_r}. \tag{24}$$

This can be proven[29] by substituting the values for the left eigenvectors (24) in the corresponding left eigenvalue problem formulation (22) and by transposing the matrix equation. Based on the assumption of symmetry of both the structural and the acoustical submatrices A^s and A^f, this indeed yields the right eigenvalue problem with the corresponding right eigenvectors. This leads to the following conclusions about the modal description of the coupled vibro-acoustical system, which are in correspondence with those drawn by Zhang.[17]

The transfer functions between structural displacement x_i at location i or acoustical pressure response p_l at location l, and structural force excitation f_j at location j can be written as a function of the right eigenvectors and eigenvalues of the system matrix, as follows, based upon Eqs. (18), (19), (22), (23), and (24):

$$\frac{x_i}{f_j} = \sum_{r=1}^{N} \frac{P_r\psi_{sri}\psi_{srj}}{(s-\lambda_r)} + \frac{(P_r\psi_{sri}\psi_{srj})^*}{(s-\lambda_r^*)}, \tag{25}$$

$$\frac{p_l}{f_j} = \sum_{r=1}^{N} \frac{P_r\psi_{frl}\psi_{srj}}{(s-\lambda_r)} + \frac{(P_r\psi_{frl}\psi_{srj})^*}{(s-\lambda_r^*)}. \tag{26}$$

The transfer functions between structural displacement x_i at location i or acoustical pressure response p_l at location l and acoustical volume acceleration excitation $\dot{q}_k$ at location k can be written as follows:

$$\frac{x_i}{\dot{q}_k} = \sum_{r=1}^{N} \frac{P_r\psi_{sri}\psi_{frk}}{\lambda_r^2(s-\lambda_r)} + \frac{(P_r\psi_{sri}\psi_{frk})^*}{\lambda_r^2(s-\lambda_r^*)}, \tag{27}$$

$$\frac{p_l}{\dot{q}_k} = \sum_{r=1}^{N} \frac{P_r\psi_{frl}\psi_{frk}}{\lambda_r^2(s-\lambda_r)} + \frac{(P_r\psi_{frl}\psi_{frk})^*}{\lambda_r^2(s-\lambda_r^*)}. \tag{28}$$

The right eigenvectors of the coupled problem represent (but for a global scale factor) the vibro-acoustical modes; the left eigenvectors represent (but for a scale factor per mode) the participation factors. Due to the special relation between left and right eigenvectors, the participation factors for acoustical excitation and structural excitation are different with a scale factor that equals the eigenvalue squared (and thus different from mode to mode).

It is interesting to point out that Eqs. (26) and (27) for $l=k$ and $j=i$ reflect the vibroacoustical reciprocity relationship. This requires

$$\frac{p_k}{f_i} = -\frac{\ddot{x}_i}{\dot{q}_k} \tag{29}$$

or

$$\sum_{r=1}^{N} \frac{P_r\psi_{frk}\psi_{sri}}{(s-\lambda_r)} + \frac{(P_r\psi_{frk}\psi_{sri})^*}{(s-\lambda_r^*)} = -s^2\left(\sum_{r=1}^{N} \frac{P_r\psi_{sri}\psi_{frk}}{\lambda_r^2(s-\lambda_r)} + \frac{(P_r\psi_{sri}\psi_{frk})^*}{\lambda_r^2(s-\lambda_r^*)}\right). \tag{30}$$

One can see that for *individual* modes (considering individual terms in the above summation) the vibro-acoustical relationship does not hold (as unlike for purely structural or acoustical systems). Per mode, a frequency-dependent factor $(-\lambda_r^2/s^2)$ is causing the nonreciprocity. However, for the summed contribution of all active modes into a frequency response function, the vibro-acoustical reciprocity is complied with. This illustrates the importance of truncation effects when synthesizing a frequency response function from a *limited* number of vibro-acoustical modes.

IV. IMPLICATIONS FOR EXPERIMENTAL VIBRO-ACOUSTICAL MODAL ANALYSIS

Most of the multiple input/multiple output modal parameter estimation algorithms do not require symmetry. The nonsymmetry of the basic set of equations (14), and hence of the modal descriptions (25)–(28), does not pose, as such, any problems for those parameter estimation techniques, in order to obtain valid modal frequencies and damping factors. Considering that mode shapes themselves are arbitrarily scaled vectors, the same also holds for mode shapes. However, in an actual implementation for vibro-acoustical modal analysis, care must be taken to handle mixed structural and acoustical frequency response functions in terms of both units and absolute levels.

For practical applications, structural excitation can be substituted by acoustical excitation [see Eqs. (25)–(28)]. This is often preferred for different reasons: placing an acoustical source is usually more practicable than placing a shaker; the acoustics of the cavity, which is the goal function to be studied, is excited in a direct way; the measurements

are more efficient. However, there is a very important practical aspect: how to determine the quantity $\dot{q}$ (volume acceleration) of the acoustical source. Various calibration techniques have been suggested[30] and are in use with success for quite some time. (The methods used for the application part in this paper will be discussed in Sec. V B.) The modal models (mode shapes, frequencies, and damping factors) derived from either acoustical excitation frequency response functions (FRFs) or structural excitation FRFs are compatible.

However, it is imperative to bear in mind that the participation factors obtained with acoustical excitation differ by a scale factor per mode, as related to the structural excitation, due to the special nonsymmetry of the set of equations. This has its consequences if the obtained modal model is used for further calculations; for example, in expanding the system matrix from one type of excitation to another. For purely structural applications, the expansion is symmetrical, based on the structural reciprocity principle. In vibro-acoustical systems, the expansion must be done according to the vibro-acoustical reciprocity principle, which means the expansion from one excitation type to the other cannot be done in a symmetrical way. This is reflected in the scale factors that must be applied in order to go from the structural formulations (25) and (26) to the acoustical formulations (27) and (28). Furthermore, since the scaling factors are the squared eigenvalues, they are different for each considered mode. An application of these principles is demonstrated in Sec. V F.

V. APPLICATION: MEASUREMENTS AND ANALYSIS ON A VIBRO-ACOUSTICAL MODEL

The extension of the traditional experimental modal analysis tools and techniques of mechanical systems to vibro-acoustical systems is demonstrated and verified on the basis of an extensive measurement series, performed on a simple vibro-acoustical measurement setup. The main goal of the reported experiments is to prove the applicability and usefulness of combination of mechanical and acoustical excitations and responses in complex systems, but none the less to draw attention to some critical points which can be crucial in some applications.

A. Model description

The model used for the experiments is an irregular polyvinylchloride (PVC) box (with some resemblance to a car body) of maximum dimension 0.84×0.4×0.4 m, plate thickness 0.01 m. The box can either be closed with a PVC bottom plate (for the uncoupled acoustical case) or with a flexible steel plate of 0.001 m thickness (for the vibro-acoustical coupled case). A third possible version of this setup can be obtained by removing the three top plates, thus bringing about nearly uncoupled conditions for the flexible bottom plate (uncoupled structural case).

The acoustical excitation is ensured by a loudspeaker provided with a closed back cavity, built in one of the upper corners of the model box. It can be taken out and replaced by a rigid PVC plate during the structural excitation measurements in order to close the cavity with uniform impedance everywhere and enable one to measure the blocked pressure

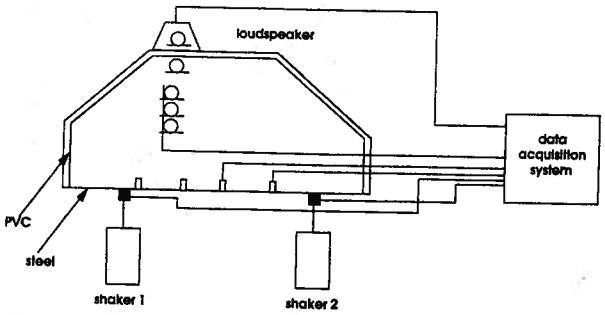

FIG. 1. Experimental setup.

as required by Eq. (11). For the structural excitation an impact hammer or two shakers are used; these latter ones decoupled during the acoustical excitation experiments, again in order to avoid any uncontrolled impedance constraints. The references for the structural excitation are measured by force transducers; the structural responses are measured by means of a set of roving accelerometers. The reference for the acoustical excitation, i.e., volume acceleration of the acoustical source, was derived from the input voltage to the loudspeaker (to be discussed in Sec. V B in more detail). The acoustical responses were measured by means of a roving array of five miniature electret microphones. The total number of structural responses was 212, the number of acoustical responses was 151 (including driving point measurements). Figure 1 shows the experimental setup.

B. Acoustical source calibration

The correct calibration of the acoustical source is essential if one aims at proving vibro-acoustical reciprocity in quantitative terms. The acoustical source is calibrated by laser velocity measurements at 31 points on the loudspeaker surface in the form of FRFs referenced to the input voltage, and this under anechoic conditions in a frequency range 20–500 Hz. The volume acceleration versus input voltage calibration function is then calculated as the average velocity over all points, multiplied by the active surface of the diaphragm of the loudspeaker and $j\omega$. Figure 2 shows the obtained calibration curve used throughout the measurement series.

In order to establish whether or not the loudspeaker's output is unacceptably influenced by the loading impedance of the cavity during the actual measurements, the pressure in the back cavity of the loudspeaker referenced to the input voltage is measured as well, both during calibration and during the actual measurement runs. Figure 3 shows the superposition of the back cavity pressure/voltage FRF during calibration (under free field conditions) and during measurement (loudspeaker in enclosed cavity). Clearly, the effects of the acoustical resonances of the cavity can be seen, but are nevertheless negligible. This implies that the input voltage of the loudspeaker can be considered as a correct reference signal for the measurements.

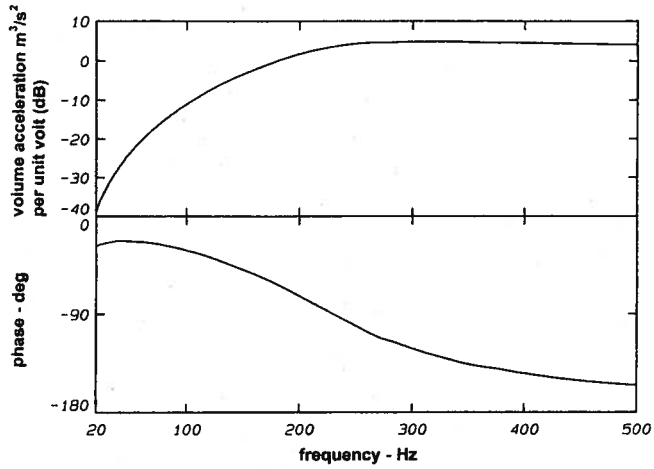

FIG. 2. Calibration curve of the used loudspeaker: FRF of the radiated volume acceleration referenced to the input voltage.

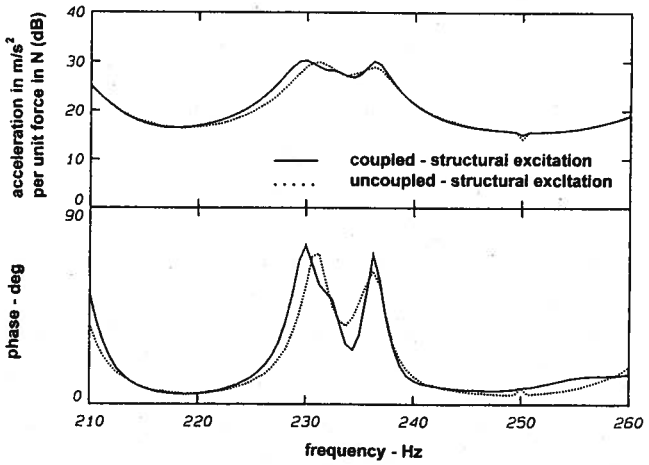

FIG. 4. Effect of coupling on the structural response, expressed by the average FRF of the plate accelerations referenced to one of the external force inputs for the coupled (solid curve) and the uncoupled case (dashed curve).

C. Measurements

In order to establish the effects of vibro-acoustical coupling on the modal characteristics of the various systems investigated, three series of measurements are performed: one to reveal the characteristics of the flexible bottom plate of the box without cavity (uncoupled structural subsystem—(dual input) structural excitation, structural responses); one to determine the modal model of the cavity enclosed with rigid walls (uncoupled acoustical subsystem—(single input) acoustical excitation, acoustical responses); and eventually, measurements on the coupled vibro-acoustical system (both structural and acoustical responses). In the course of the measurements series, only auto- and cross-powers were measured and stored. The calculations of the FRFs and the modal analysis were performed subsequently.

Figure 4 gives the arithmetic average of all 212 measured structural FRFs (structural response per structural excitation) for both the uncoupled and coupled case, between 210 Hz and 260 Hz (232 Hz is the first acoustical cavity mode). Figure 5 gives the average acoustical/acoustical FRFs (calculated anologously to its structural counterpart) for both the uncoupled and coupled case. It is clear from Fig. 5 that the acoustical response in the cavity is remarkably affected by the coupling. New resonance frequencies emerge, while the original (uncoupled) resonance frequency essentially remains unchanged. The structural response is less sensitive, even though a thorough analysis shows the existence of a new peak in the data in the coupled case. A small shift of the original resonance frequencies can also be observed. A more detailed analysis of the measured results is given in Sec. V E.

It is worthwhile to note at this point that although coupling resulted in some slight shifts in resonance frequencies (which is fully consistent with theoretical considerations), similar frequency differences were also encountered between modal analyses by using different excitation techniques. These latter variations lended themselves to an explanation by the loading effect of the applied force cells when using

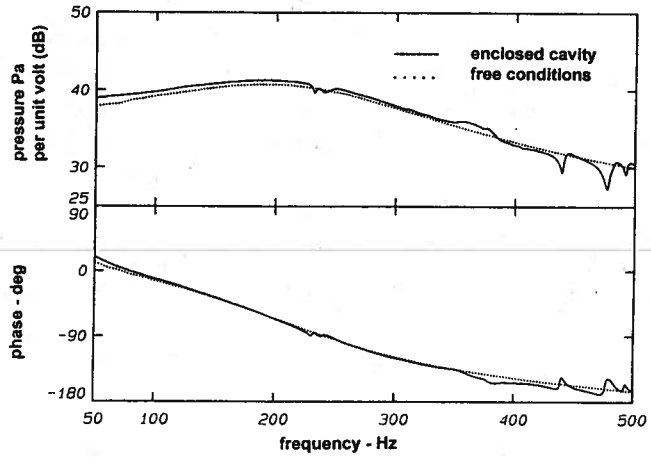

FIG. 3. Loading effect of the cavity on the loudspeaker's source strength: FRF of the back cavity pressure of the loudspeaker, referenced to its input voltage under free field conditions (dashed curve), and placed in the cavity (solid curve).

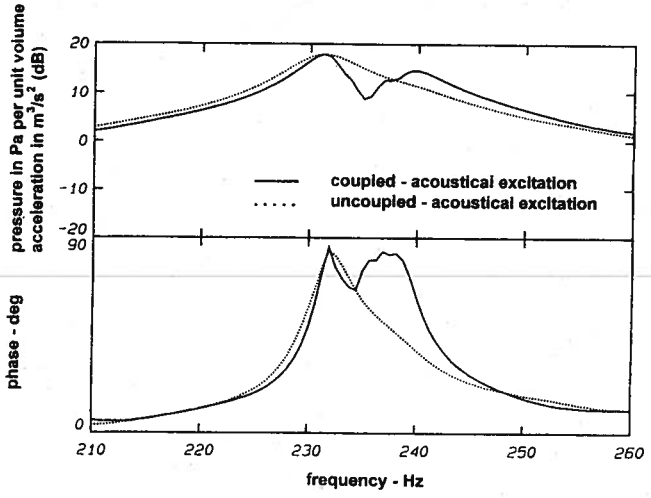

FIG. 5. Effect of coupling on the fluid response, expressed by the average FRF of the sound pressures referenced to the input volume acceleration of the loudspeaker for the coupled (solid curve) and the uncoupled case (dashed curve).

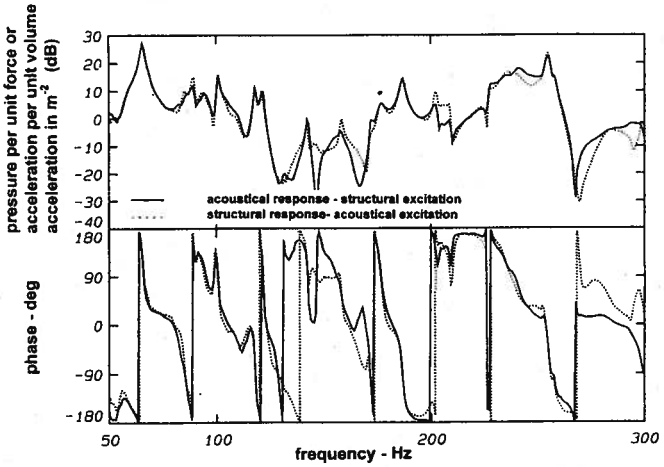

FIG. 6. Vibro-acoustical reciprocity at force input location 1, hammer excitation: acoustical/structural FRF (solid curve) and structural/acoustical FRF (dashed curve).

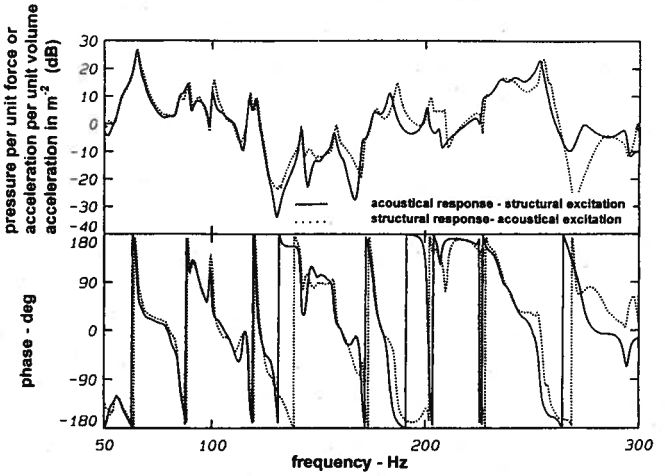

FIG. 7. Vibro-acoustical reciprocity at force input location 1, shaker excitation: acoustical/structural FRF (solid curve) and structural/acoustical FRF (dashed curve).

shakers for the structural excitation, thus they do not contradict those conclusions drawn in Sec. IV. A further factor, mostly not essential in the analysis of pure mechanical systems but often deteriorating the accuracy of extensive vibro-acoustic experiments, is the variation of air temperature in the course of the measurements, resulting in continuously changing sound speed and therefore changing resonance frequencies. In spite of every effort to keep measurement time as low as possible, the measurements had to be performed over the course of several days.

D. Vibro-acoustical reciprocity

Due to the absolute calibration of the acoustical source used in the experiment, the vibro-acoustical reciprocity can be fully verified in quantitative terms. Figure 6 shows the superposition of two FRFs; one being the acoustical pressure response at the loudspeaker's location (with the loudspeaker taken away from the measurement setup and substituted by a rigid plate) with respect to structural excitation at one position obtained by impact hammer excitation, and the other being an acceleration response at this force input position with respect to acoustical excitation of the loudspeaker. As one can see, apart from some low-level notches and narrow frequency regions, the agreement between the two measurements is quite reasonable, showing that vibro-acoustical reciprocity is a valid assumption for this experimental system. Note that the agreement is considerably worse if shaker input measurements are used, obviously distorted by a small but not negligible load effect of the top housing of the applied force sensor (Fig. 7).

Not surprisingly, deviations also become more pronounced with increasing frequencies. The supposed reason of this disagreement is that the basic assumption of the vibro-acoustic reciprocity principle, namely that the considered acoustical source is an ideal omnidirectional monopole, is more difficult to realize at higher frequencies. The discrepancy stresses the need for a new generation of calibrated acoustical volume velocity sources for this sort of applications.

E. Modal analysis results

Using the measured acoustical, structural, structural/acoustical, and acoustical/structural FRFs for both the coupled and uncoupled cases, four sets of modal analyses were performed in total.

Standard least-squares complex exponential and least-squares frequency domain curve fitting procedures were used for curve fitting all available data.[28] This resulted in the modal frequencies and damping factors for the different cases considered; a few of them are reported in Table I. The number of modal frequencies is increased in the considered band and slight frequency shifts can be observed, as discussed in Sec. V C and Sec. V D.

Figure 8(a)–(d) show the uncoupled acoustical and uncoupled structural mode shapes, as well as the corresponding coupled vibro-accoustical mode shapes, estimated from structural as well as acoustical excitation. Similar to the structural ones, the visualization of the acoustical mode shape of the cavity is done by a "displacement" perpendicular to the wireframe planes along which the sound pressures were measured. Clearly, vibro-acoustical coupling has little effect on the uncoupled mode shapes, and both the structural and acoustical coupled mode shapes are essentially identical, irrespective of whether the system is structurally or acoustically excited. This verifies the theoretical considerations that the derivation of a vibro-acoustical modal model is independent from the applied inputs.

TABLE I. Estimated modal frequencies and damping ratios for various (uncoupled and coupled) systems in the frequency range around the first acoustical cavity resonance.

Uncoupled acoustical subsystem	Uncoupled structural subsystem	Coupled vibro-acoustic system, structural excitation	Coupled vibro-acoustic system, acoustical excitation
	230.9 Hz/0.8%	230.0 Hz/0.7%	231.8 Hz/0.7%
230.9 Hz/1.4%		232.6 Hz/0.6%	233.6 Hz/0.5%
	236.4 Hz/0.6%	236.3 Hz/0.5%0	237.2 Hz/0.5%
		238.1 Hz/0.9%	238.4 Hz/1.0%

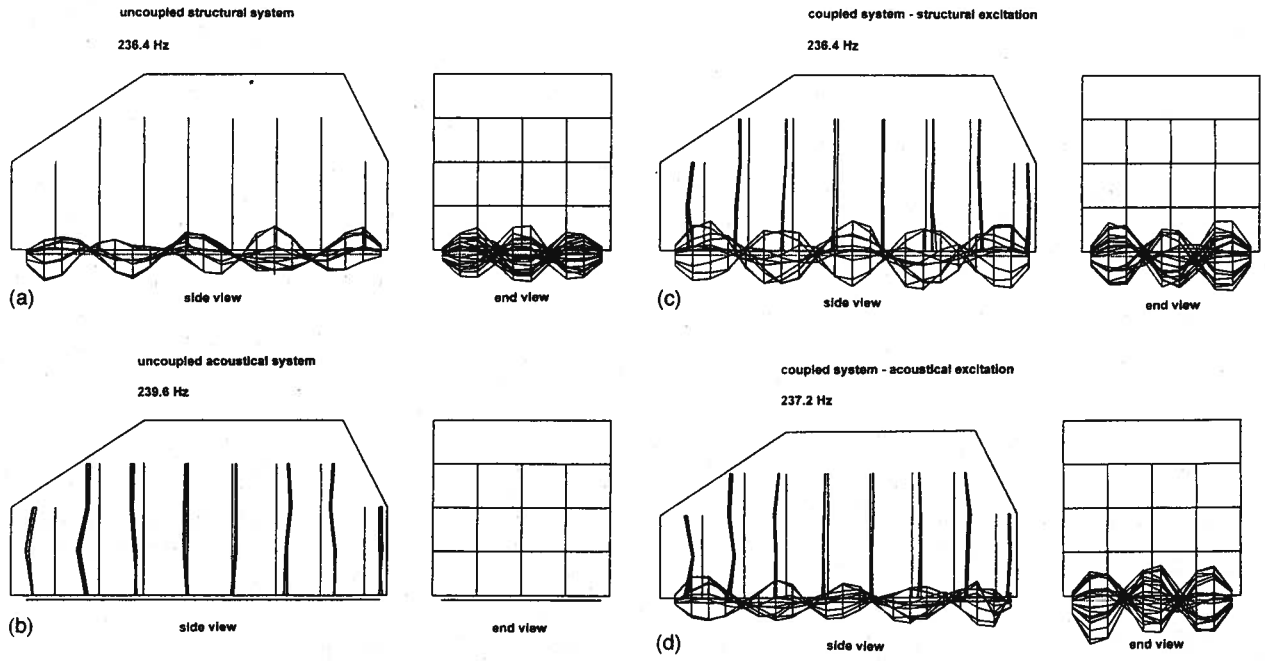

FIG. 8. Modal deformations: (a) uncoupled structural case; (b) uncoupled acoustical case; (c) coupled vibro-acoustical case: structural excitation; (d) coupled vibro-acoustical case: acoustical excitation.

F. FRF synthesis in vibro-acoustical systems

Unlike the derivation of a modal model itself, its use for further calculations is not as straightforward and the non-symmetry of the modal formulation may no longer be disregarded. The similarities and the differences in the application of a vibro-acoustical modal model is demonstrated in the framework of an FRF synthesis exercise.

Since the applied modal formalism, Eq. (9) is an extension of, and thus fully compatible with, that of a purely mechanical system, the classical frequency response matrix methods of the experimental modal analysis method may also be applied. Using Eq. (15), one can rewrite Eqs. (14) in the simple form

$$[H]\begin{Bmatrix} f \\ \dot{q} \end{Bmatrix} = \begin{Bmatrix} \ddot{x} \\ p \end{Bmatrix}. \tag{31}$$

Just as in the case of purely mechanical systems, the full frequency response matrix H which is made of $d \times d$ FRFs (where d denotes the sum of the measured structural and acoustical degrees of freedom) can be constructed from one single row or column of d measured frequency response functions. This implies that, based on the modal parameters estimated from frequency response functions measured with reference to one single structural or acoustical input, it is possible to synthesize frequency response functions with respect to any other input, irrespective of its kind or location. (The necessary conditions of this synthesis are that a complete column of the FRF matrix is available and the d FRFs must contain nonzero residue information for every modal vector.) For purely structural applications, this synthesis is based on symmetrical extrapolation. For vibro-acoustical applications, the extrapolation from one type of excitation to the other type of excitation requires a vibro-acoustical reciprocal extrapolation, which is not symmetrical. The synthesis of an acoustical response, for instance, due to structural excitation at a given location, can be done based on the modal model obtained via acoustical excitation, with inclusion of the proper scaling of the mode shapes. If this scaling is not taken into account, the obtained synthesis will not be correct.

As an example, assume now that the synthesis of the FRF between a sound pressure at point k and a force at point m is desired, provided that a modal model is available which is based on a full set of FRFs measured with respect to acoustical excitation at location t. According to Eq. (18), the sought element of the FRF matrix, p_k/f_m, can be expressed as a sum of N modal contributions

$$H_{km} \equiv \frac{p_k}{f_m} = \sum_{r=1}^{N} \frac{A_{rkm}}{(s-\lambda_r)} + \frac{A^*_{rkm}}{(s-\lambda^*_r)}. \tag{32}$$

Each contribution is described by the eigenvalue λ_r and the appropriate element of the residue matrix, A_{rkm}. This element can be described as, according to Eq. (26),

$$A_{rkm} = P_r \psi_{frk} \psi_{srm} = \frac{P_r \psi_{frk} \psi_{srt} P_r \psi_{frt} \psi_{srm}}{P_r \psi_{frt} \psi_{srt}}$$

$$= A_{rkt} \frac{1}{A_{rtt}} A_{rtm}. \tag{33}$$

Given all elements of the tth column of the residue matrix (FRFs with respect to acoustical excitation in t available), the first and second product terms in Eq. (33) are readily available. Nevertheless, the third term describing the acoustical modal response at location t due to the structural excitation at location m can be calculated by making use of the vibro-acoustical reciprocity relation, taking the structural response at m due to the acoustical excitation at t. Based on Eqs. (26) and (27), the needed residue is obtained from

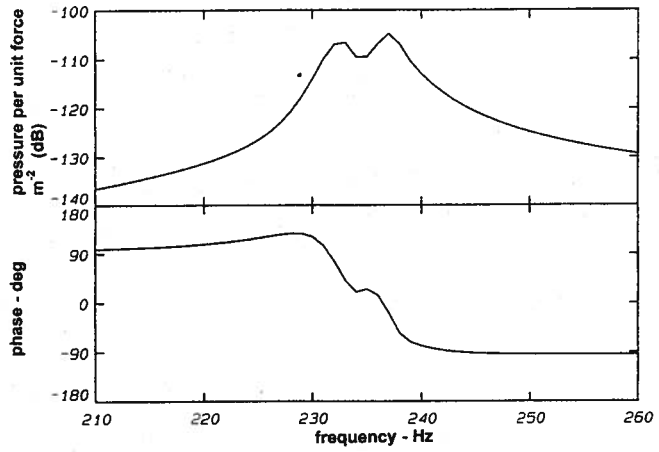

FIG. 9. Synthesis of acoustical response/structural excitation FRF based on a nonscaled acoustical excitation modal model.

$$A_{rtm} = \lambda_r^2 A_{rmt}. \tag{34}$$

Substituting Eqs. (34) and (33) back to Eq. (32) and performing the summation for all considered modes, one ends up with the desired FRF. One should certainly remain aware of the importance of truncation by taking only a limited number of modes on the vibro-acoustical reciprocity relationship as mentioned in Sec. III.

Figure 9 shows the FRF synthesized without appropriately scaling the acoustical excitation modal model, before expanding it to the structural excitation case; Fig. 10 shows the resulting FRF with appropriate scaling. Clearly, large scaling deviations (130 dB) exist between the two synthesized FRFs. Figure 11 then shows the synthesized FRF from the structural excitation modal model. The differences in Figs. 10 and 11 are mainly due to the shift in modal frequencies that were observed during the tests. At resonance the magnitude of the FRFs are corresponding quite well. Off-resonance, the deviations are larger due to the aforementioned truncation effects.

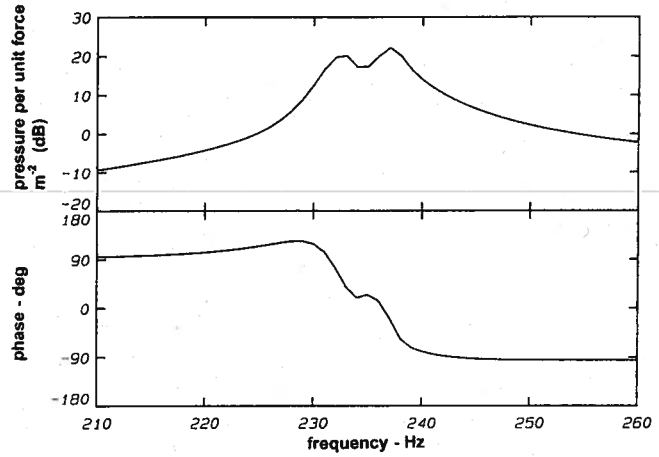

FIG. 10. Synthesis of acoustical response/structural excitation FRF based on a scaled acoustical excitation modal model.

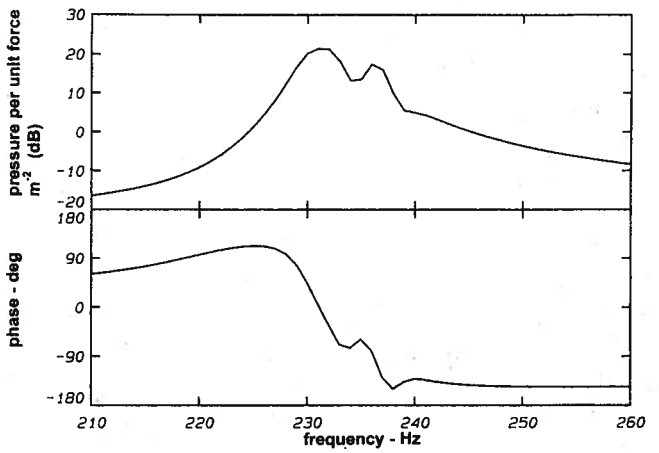

FIG. 11. Synthesis of acoustical response/structural excitation FRF based on a structural excitation modal model.

VI. CONCLUSIONS

Within this paper a framework of reference has been put down for performing vibro-accoustical modal analysis. Starting from a theoretical finite element formulation of the vibro-acoustical problem, it is shown which second-order model formulation is appropriate and consistent for experimental vibro-acoustical modal analysis. It is explained which physical parameters must be measured, both in the case of structural excitation and in the case of acoustical excitation. Also, it is shown that the general vibro-acoustical reciprocity does not imply model symmetry. The consequence of this is that a special modal scaling, equal to the eigenvalues squared, must be applied in the modal models to go from acoustical excitation to structural excitation, and vice versa.

The theory is proven by performing extensive structural and acoustical tests, both using structural and acoustical excitation, on a laboratory model. Care is taken to calibrate the acoustical source strength. By doing this, vibro-acoustical reciprocity can be verified and proven experimentally. Consistent modal models are derived from the FRFs obtained with structural and acoustical excitation. The need for scaling the modal models when going from one type of excitation to another is demonstrated.

ACKNOWLEDGMENTS

The authors want to thank Jan Dessein for his involvement in the measurements, which were carried out with a great deal of tedious patience. They would also like to thank Jean-Pierre Coyette and Peter Göransson for valuable discussions and comments.

[1] A. J. Pretlove, "Free vibrations of a rectangular panel backed by a closed rectangular cavity," J. Sound Vib. 2(3), 197–209 (1965).
[2] E. H. Dowell and H. M. Voss, "The effect of a cavity on panel vibration," AIAA J. 1, 476–477 (1963).
[3] R. H. Lyon, "Noise reduction of rectangular enclosures with one flexible wall," J. Acoustic. Soc. Am. 35, 1791–1797 (1973).
[4] R. W. Guy and M. C. Bhattacharya, "The transmission of sound through a cavity-backed finite plate," J. Sound Vib. 27, 207–223 (1973).
[5] E. H. Dowell, G. F. Gorman III, and D. A. Smith, "Acoustoelasticity: General theory, acoustical natural modes, and forced response to sinu-

soidal excitation, including comparisons with experiment," J. Sound Vib. **52**, 519–542 (1977).
[6] J. Pan and D. A. Bies, "The effect of fluid-structural coupling on sound waves in an enclosure: Theoretical part," J. Acoust. Soc. Am. **87**, 691–707 (1990).
[7] J. Pan and D. A. Bies, "The effect of fluid-structural coupling on sound waves in an enclosure: Experimental part," J. Acoust. Soc. Am. **87**, 708–717 (1990).
[8] P. Göransson, "Acoustic finite elements," in *Advanced Techniques in Applied and Numerical Acoustics*, edited by P. Sas (K. U. Leuven, 1993), Part VI.
[9] J.-P. Coyette, "Acoustic boundary elements," in *Advanced Techniques in Applied and Numerical Acoustics*, edited by P. Sas (K. U. Leuven, 1993), Part VIII.
[10] D. L. Smith, "Experimental techniques for acoustical modal analysis of cavities," Proc. Inter-Noise 76, Washington, DC, 5–7 April 1976, pp. 129–132.
[11] J. J. Nieter and R. Singh, "Acoustic modal analysis experiment," J. Acoust. Soc. Am. **72**, 319–326 (1982).
[12] D. L. Brown and R. J. Allemang, "Modal analysis techniques applicable to acoustical problem solution," Proc. Inter-Noise 78, San Francisco, 8–10 May 1978, pp. 909–914.
[13] F. Augusztinovicz, "Acoustic modal analysis," in *Advanced Techniques in Applied and Numerical Acoustics*, edited by P. Sas (K. U. Leuven, 1993), Part VII.
[14] J. A. Wolf, "Modal synthesis for combined structural-acoustical systems," AIAA J. **15**, 743–745 (1977).
[15] D. J. Nefske and S. H. Sung, "Structural-acoustical system analysis using the modal synthesis technique," Proc. 3rd Int. Modal Analysis Conf., Orlando, 28–31 January 1985, pp. 864–868.
[16] V. B. Bokil and U. S. Shirahatti, "A technique for the modal analysis of sound–structure interaction problems," J. Sound Vib. **173**, 23–41 (1994).
[17] Q. Zhang, "Application de l'analyse modale à la résolution des problèmes acoustiques automobiles en basses fréquence," J. Soc. Ing. Automobile **380**, 44–50 (1993).
[18] L. M. Lyamshev, "A question in connection with the principle of reciprocity in acoustics," Sov. Phys. Dokl. **4**, 406–409 (1959).
[19] T. ten Wolde, J. W. Verheij, and H. F. Steenhoek, "Reciprocity method for the measurement of mechano-acoustical transfer functions," J. Sound Vib. **42**, 49–55 (1975).
[20] F. J. Fahy, "The reciprocity principle and applications in vibro-acoustics," Proc. Inst. Acoust. **12** (part 1), 1–20 (1990).
[21] A. N. Norris and D. A. Rebinsky, "Acoustic reciprocity for fluid–structure problems," J. Acoust. Soc. Am. **94**, 1714–1715 (1993).
[22] V. Easwaran, V. H. Gupta, and M. L. Munjal, "Relationship between the impedance matrix and the transfer matrix with specific reference to symmetrical, reciprocal, and conservative systems," J. Sound Vib. **161**, 515–525 (1993).
[23] J. W. Verheij, "A comment on the relationship between reciprocal and symmetrical systems," J. Sound Vib. **170**, 567–570 (1994).
[24] H. V. Gupta, "On independence of reciprocity, symmetry and conservativeness of one-dimensional linear systems," J. Sound Vib. **179**, 547–552 (1995).
[25] G. C. Everstine, "A symmetrical potential formulation for fluid–structure interaction," J. Sound Vib. **79**, 157–160 (1981).
[26] A. Kanarachos and I. Antoniadis, "Symmetric variational principles and modal methods in fluid–structure interaction problems," J. Sound Vib. **121**, 77–104 (1988).
[27] G. Sandberg and P. Göransson, "A symmetrical finite element formulation for acoustical fluid–structure interaction analysis," J. Sound Vib. **123**, 507–515 (1988).
[28] W. Heylen, P. Sas, and S. Lammens, "Modal analysis theory and testing," in *Proceedings of the 18th International Seminar on Modal Analysis*, edited by P. Sas (K. U. Leuven, 1993), Part I.
[29] Z.-D. Ma and I. Hagiwara, "Sensitivity analysis methods for coupled acoustical-structural systems. Part I: Modal sensitivities," AIAA J. **29**, 1787–1795 (1991).
[30] R. Singh and M. Schary, "Acoustic impedance measurement using sine sweep excitation and known volume velocity technique," J. Acoust. Soc. Am. **64**, 995–1003 (1978).
[31] I. L. Vér, "Use of reciprocity and superposition as a diagnostic and design tool in noise control," Acta Acustica **82**, DAGIFS (1996).